J. Fluid Mech. (1975), *vol.* 72, *part* 4, *pp.* 605–623
Printed in Great Britain

Closed-streamline flows past rotating single cylinders and spheres: inertia effects

By G. G. POE† AND ANDREAS ACRIVOS
Department of Chemical Engineering, Stanford University, Stanford, California 94305

(Received 21 April 1975)

The flow around a cylinder and a sphere rotating freely in a simple shear was studied experimentally for moderate values of the shear Reynolds number Re. For a freely rotating cylinder, the data were found to be consistent with the results obtained numerically by Kossack & Acrivos (1974), at least for Reynolds numbers up to about 10. Rates of rotation of a freely suspended sphere were also obtained over the same range of Reynolds numbers and showed that, with increasing Re, the dimensionless angular velocity does not decrease as fast for a sphere as it does for a cylinder. In both cases, photographs of the streamline patterns around the objects were consistent with this behaviour. Furthermore, it was found in each case that the asymptotic solutions for $Re \ll 1$ derived by Robertson & Acrivos (1970) for a cylinder and by Lin, Peery & Schowalter (1970) for a sphere are not valid for Reynolds numbers greater than about 0·1, and that the flow remains steady only up to values of Re of about 6.

1. Introduction

A thorough understanding of the behaviour of small cylinders and spheres freely suspended in non-uniform flow fields is essential to the solution of many complex problems in suspension rheology. However, much of the experimental as well as the theoretical effort on this subject has been devoted to small values of the Reynolds number, thus leaving virtually unexplored the many effects resulting from the presence of large inertia forces in the system. In fact, in the case of steady linear shear flows, these inertia effects appear to have been considered by only a few investigators, for example Bretherton (1962), Saffman (1965), Robertson & Acrivos (1970), Lin *et al.* (1970) and, most recently, Kossack & Acrivos (1974).

The present study is an experimental investigation of the angular velocity and streamline patterns for both a circular cylinder and a small sphere each freely suspended and each placed symmetrically in a steady simple shear for values of the shear Reynolds number Re up to about 10. Robertson & Acrivos (1970) and Lin *et al.* (1970) treated this problem theoretically for $Re \ll 1$. For the case of a cylinder, Robertson & Acrivos obtained the first-order correction term to the creeping-flow solution using the well-known technique of inner and outer

† Present address: Aerotherm Division of Acurex Corporation, Mountain View, California 94042.

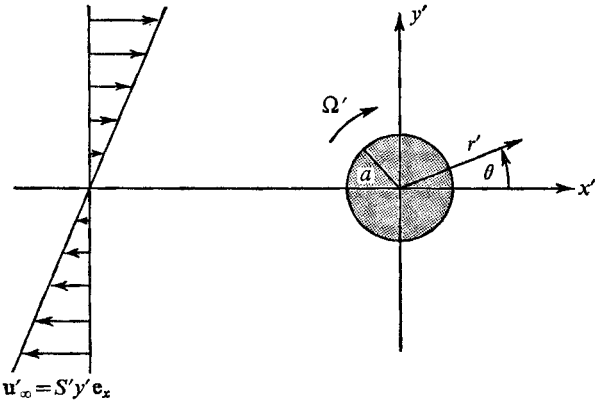

FIGURE 1. The unperturbed velocity field and the location of the cylinder or sphere in the flow (z' axis directed outward).

expansions, while Lin *et al.* (1970) derived in a similar manner the corresponding solution for a sphere.

Since most experimental studies reported to date have been confined to values of Re low enough for inertia effects to be negligible, it was felt that an experimental investigation of this problem for values of Re beyond the Stokes range was warranted. Owing to the appearance of flow instabilities, however, steady-flow experiments could be performed for Re only as high as about 10. None the less, the present study was undertaken in an attempt to determine the range of validity of the two previously mentioned asymptotic solutions as well as to obtain some insight into the effects of inertia for moderate Re. Since it was relatively easy to measure the angular velocity of a freely suspended cylinder or sphere immersed in a simple shear, this was the primary variable used in comparing the present experimental results with the two asymptotic solutions. In addition, the data obtained here for the cylinder provided experimental confirmation of some of the theoretical results of Kossack & Acrivos (1974), who presented complete numerical solutions to the full two-dimensional Navier–Stokes equations for values of Re up to 70. Of course, since numerical solutions to the full equations for a sphere have not been obtained as yet, a comparison could not be made in this instance. Thus the changes with increasing Re in the angular velocity and in the streamline patterns observed here for a sphere constitute one of the major original results of this study.

The physical system consists of an incompressible Newtonian fluid in steady simple shear flow past a neutrally buoyant, freely suspended cylinder or sphere. As depicted in figure 1, the cylinder or sphere (of radius a) is placed symmetrically in the shear flow and is allowed to rotate about the z' axis with angular velocity $\boldsymbol{\Omega}' = \Omega' \mathbf{e}_z$, $\mathbf{e}_k$ denoting a unit vector along the $\mathbf{k}$ co-ordinate axis. The undisturbed fluid velocity is taken to be $\mathbf{u}'_\infty = S'y'\mathbf{e}_x$, where S' is the impressed constant rate of shear. The particle shear Reynolds number Re is then defined as $Re \equiv \rho S'a^2/\mu$, ρ being the density and μ the viscosity of the fluid. In terms of the dimensionless quantities

$$\mathbf{r} \equiv \mathbf{r}'/a, \quad \mathbf{u} \equiv \mathbf{u}'/S'a, \quad p \equiv p'/S'\mu, \quad \boldsymbol{\Omega} \equiv \boldsymbol{\Omega}'/S', \quad \Omega \equiv \Omega'/S',$$

the steady Navier–Stokes equations in Cartesian co-ordinates take the form

$$\nabla.\mathbf{u} = 0, \quad Re\,\mathbf{u}.\nabla\mathbf{u} = -\nabla p + \nabla^2\mathbf{u}, \tag{1.1a,b}$$

with boundary conditions

$$\mathbf{u} = -\boldsymbol{\Omega}\times\mathbf{r} = \Omega(y\mathbf{e}_x - x\mathbf{e}_y) \quad \text{at} \quad |\mathbf{r}| = 1, \tag{1.2a}$$

$$\mathbf{u} \to y\mathbf{e}_x, \quad p \to 0 \quad \text{as} \quad |\mathbf{r}| \to \infty, \tag{1.2b}$$

where, for a freely suspended particle, Ω is determined by the condition of zero torque. The primary aim of the present study was to obtain experimentally the dependence of Ω on Re and to photograph the streamline patterns in the vicinity of both a cylinder and a sphere for values of Re up to about 10. Before proceeding with a description of the shear-flow apparatus and the experimental programme, though, we discuss some of the important results from earlier studies so that a more meaningful comparison can be made with the present experimental findings.

In treating the cylinder problem mathematically, it is convenient to use cylindrical co-ordinates r and θ (see figure 1) and to express the solution in terms of the two-dimensional stream function ψ defined by

$$u_r = r^{-1}\partial\psi/\partial\theta, \quad u_\theta = -\partial\psi/\partial r.$$

Thus the steady Navier–Stokes equations and boundary conditions (1.1) and (1.2) become

$$\frac{Re}{r}\left(\frac{\partial\psi}{\partial\theta}\frac{\partial\nabla^2\psi}{\partial r} - \frac{\partial\psi}{\partial r}\frac{\partial\nabla^2\psi}{\partial\theta}\right) = \nabla^4\psi, \tag{1.3}$$

$$\psi = 0, \quad \partial\psi/\partial r = \Omega \quad \text{at} \quad r = 1, \tag{1.4a,b}$$

$$\psi \to \tfrac{1}{2}r^2\sin^2\theta \quad \text{as} \quad r \to \infty. \tag{1.4c}$$

The well-known Stokes solution to (1.3) and (1.4) for zero torque, given by

$$\psi_0 = \tfrac{1}{4}(r^2-1) - \tfrac{1}{4}(r^2 - 2 + r^{-2})\cos 2\theta, \quad \Omega_0 = \tfrac{1}{2}, \tag{1.5a,b}$$

the subscript zero denoting the solution for $Re = 0$, was first presented by Raasch (1961), and the predicted flow pattern verified experimentally for very small values of Re by Darabaner, Raasch & Mason (1967), Cox, Zia & Mason (1968) and by Robertson & Acrivos (1970). The Stokes solution (1.5) predicts that streamlines are either open or closed according to whether they lie outside or inside a so-called limiting streamline (cf. Cox *et al.* 1968). Theoretically, when $Re \equiv 0$, the extent of this closed-streamline region is infinite. However, as pointed out by Robertson & Acrivos, the existence of a region of closed streamlines at distances far from the cylinder contradicts the uniform-shear boundary condition at infinity. Thus, in order to obtain a smooth transition between the flow near the cylinder and that far from the body, the inertia terms in (1.3) must somehow be properly taken into account. Robertson & Acrivos then computed the effect of fluid inertia to $O(Re)$ on the stream function ψ using the familiar technique of inner and outer expansions (cf. Proudman & Pearson 1957) and obtained a solution to (1.3) and (1.4) valid for small but finite Re. The 'inner' solution, for $1 \leqslant r \leqslant O(Re^{-\frac{1}{2}})$, was given as

$$\psi = \psi_0(r,\theta) + Re\ln Re\,\psi_1(r,\theta) + Re\,\psi_2(r,\theta) + O(Re^2\ln Re), \tag{1.6a}$$

where ψ_0 is the Stokes solution (1.5a) and where the functions ψ_1 and ψ_2 are the next (higher-order) terms of the expansion (see Robertson & Acrivos for the exact expressions). Moreover, for the freely suspended case, the angular velocity Ω was found to be

$$\Omega = \Omega_0[1 - 0{\cdot}2886Re + O(Re^2 \ln Re)], \tag{1.6b}$$

where $\Omega_0 = \frac{1}{2}$. This expression clearly indicates that the inclusion of inertia effects in the analysis leads to a rotation rate lower than that given by the Stokes solution (1.5b).

It is easy to show now that, if the stream function (1.6a) is evaluated for some small Re, the resulting streamline pattern will differ significantly from that of the Stokes solution. Specifically, the region of closed streamlines will be finite rather than infinite in extent and will be followed, on either side, by a recirculating wake. Also, as the Reynolds number is increased, one would expect this region of closed streamlines to become smaller and the limiting streamline to move closer to the surface of the cylinder. Indeed, this was confirmed by Kossack & Acrivos (1974), who obtained complete numerical solutions to the full equations (1.3) and (1.4) for values of Re up to 70. They found that even for moderate values of Re (~ 1) the flow is dominated by inertia effects and that its structure bears little resemblance to the solution for $Re = 0$. It is also evident from (1.6b) that Ω should be expected to decrease monotonically with Re as the Reynolds number is increased. Eventually, however, as $Re \to \infty$ under laminar flow conditions, one might expect the angular velocity to approach zero asymptotically and the cylinder to become stationary. This was borne out by the calculations of Kossack & Acrivos, who found that Ω became of order $Re^{-\frac{1}{2}}$ when $Re \geqslant 10$.

In the case of simple shear flow past a freely suspended sphere, the well-known Stokes solution to (1.1) and (1.2) is given by

$$\mathbf{u}_0 = y\left[1 - \frac{1}{2r^5} - \frac{5x^2}{2r^5}\left(1 - \frac{1}{r^2}\right)\right]\mathbf{e}_x + x\left[\frac{-1}{2r^5} - \frac{5y^2}{2r^5}\left(1 - \frac{1}{r^2}\right)\right]\mathbf{e}_y + z\left[-\frac{5xy}{2r^5}\left(1 - \frac{1}{r^2}\right)\right]\mathbf{e}_z, \tag{1.7a}$$

$$p_0 = -5xy/r^5, \quad \Omega_0 = \tfrac{1}{2}, \tag{1.7b,c}$$

the subscript zero again denoting the solution for $Re = 0$. Equation (1.7c) has been verified experimentally by Trevelyan & Mason (1951) for very small values of the Reynolds number and by Kohlman (1963) for Re up to 0·25. Also, a detailed analysis of the nature of the streamline pattern, as obtained from (1.7a), was undertaken by Cox *et al.* (1968), who found, as in the case of the cylinder, the existence of both open and closed streamlines, separated, in this case, by a limiting three-dimensional surface. These findings were then confirmed experimentally in a Couette-flow device for $Re = O(10^{-4})$.

Lin *et al.* (1970) determined, to $O(Re^{\frac{3}{2}})$, the effects of fluid inertia on the velocity and pressure fields in the vicinity of a sphere freely suspended in a simple shear. Again, the technique of inner and outer expansions was used to obtain a solution to (1.1) and (1.2) valid for small but finite Re; i.e.

$$\mathbf{u} = \mathbf{u}_0 + Re\,\mathbf{u}_1 + Re^{\frac{3}{2}}\mathbf{u}_2 + o(Re^{\frac{3}{2}}), \tag{1.8a}$$

$$p = p_0 + Re\,p_1 + Re^{\frac{3}{2}}p_2 + o(Re^{\frac{3}{2}}), \tag{1.8b}$$

where $\mathbf{u}_0$ and p_0 are the Stokes solutions (1.7*a*, *b*) and $\mathbf{u}_1$, $\mathbf{u}_2$, p_1 and p_2 are the next (higher-order) terms of the expansions (see Lin *et al.* for these expressions). In addition, from the free-suspension boundary condition (zero net force and torque), the angular velocity of the sphere was found to be

$$\Omega = \Omega_0[1 - 0{\cdot}3076 Re^{\frac{1}{2}} + o(Re^{\frac{1}{2}})], \tag{1.8c}$$

where $\Omega_0 = \frac{1}{2}$. As in the case of the cylinder, this result indicates that the inclusion of inertia effects in the analysis leads to a lowering of the rotation rate from that given by the Stokes solution (1.7*c*). Of course this is not surprising, since one would expect the solution for a sphere to behave in much the same way as that for a cylinder, the main difference being in how fast the angular velocity decreases with increasing Re. The present experimental programme will show that Ω does not decrease as fast for a sphere as for a cylinder when the Reynolds number is increased. Again, it should be noted that the inner solution (1.8) is valid only in a region near the sphere, i.e. for $1 \leqslant r \leqslant O(Re^{-\frac{1}{2}})$ as Re asymptotically approaches zero.

Since no work comparable to that of Kossack & Acrivos (1974) exists for a sphere, predictions concerning the streamline pattern for Reynolds numbers beyond the Stokes range cannot be made with certainty. However, for non-zero values of Re, one would expect the streamline pattern for a sphere, at least in the $z' = 0$ plane, to be very similar to that for a cylinder. Photographs presented below will indeed confirm this, at least for values of Re up to about 10.

A description of the shear-flow apparatus and its performance characteristics at moderate Reynolds numbers is presented in the next section. The experiments were conducted with the equipment used by Robertson (1969) in his investigation of Stokes flow around a cylinder in a simple shear. However, owing to the presence of secondary flows as well as flow instabilities, Reynolds numbers only as high as about 10 could be achieved with this device.

Section 3 contains the results of an experimental investigation of the flow around a cylinder and a sphere, each freely suspended in a steady simple shear. Photographs of the streamline patterns near the surface of the objects and measured rates of rotation are presented for Reynolds numbers in the range 0·5 to about 10. The experimental findings are then compared with the available theoretical predictions. Incidentally, streamline photos are also presented for the case $\Omega = 0$ [see (1.2*a*)], i.e. when the cylinder or sphere is stationary.

2. The shear-flow apparatus and its performance at moderate Reynolds numbers

Of the several types of device used for generating shear flows, two seem to have been used rather frequently over the past few years. One, the cylindrical Couette device, which produces a shear field in the annular region between two concentric cylinders rotating in opposite directions, has been employed quite extensively, most notably by S. G. Mason and co-workers (starting in 1951). One of the disadvantages of this type of design, however, is that the radial distribution of shear is not exactly a constant; hence, to approximate closely a constant shear

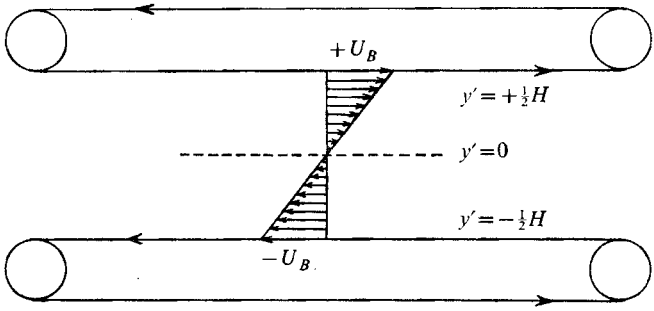

FIGURE 2. Top view of a 'parallel-band' shear-flow apparatus showing the undisturbed velocity profile.

flow, the gap between the cylinders must be so small that wall effects become significant for anything larger than microscopic particles. Thus, with this type of device, studies at Reynolds numbers beyond $O(1)$ are rather difficult to perform. On the other hand, shear-flow devices employing a 'parallel-band' design seem to be somewhat more versatile. One such example is shown schematically in figure 2. In this case, a simple shear is generated by the movement of two bands which in turn are driven by two sets of rotating pulleys at either end of the apparatus (cf. Taylor 1934; Kohlman 1963). Clearly this design has some distinct advantages over the concentric-cylinder design. For example, the shear rate between the bands is here constant, and such a device can easily be designed to provide a variable gap width without forsaking the requirement of a constant shear. However, as will presently be demonstrated, there are also several disadvantages to this 'parallel-band' type of design.

2.1. *The shear-flow apparatus*

The present experimental programme was conducted with the 'parallel-band' device used previously by Robertson & Acrivos (1970) in their investigation of Stokes flow around a cylinder in a simple shear. This apparatus consists principally of a large tank of fluid in which a system of belts and pulleys driven by two variable-speed motors is immersed. Thus a flow identical to the one depicted in figure 2 is generated. Furthermore, the entire belt and pulley assembly is supported in such a manner as to permit free movement in the transverse direction, thereby providing a continuously variable gap width. Since a great deal of flexibility was incorporated into the original design, no main modification of the equipment was required for the purposes of the present study. The only change involved the addition of two more belt supports on the outside segment of each belt in order to prevent further sagging and bowing. Details of the design and construction of the rest of the shear apparatus are described by Robertson (1969).

Before proceeding with the experimental programme, it was essential to investigate the nature of the flow between the two belts and to assess the effects of the tank geometry on the production of the experimentally measured velocity profiles while operating at Reynolds numbers beyond the Stokes range. For example, since the velocity has to be linear and two-dimensional (i.e. no vertical

velocity gradients present) over a major portion of the test channel, the effects of the end walls, the belt gap width, the belt speed, the depth of the tank, boundary layers on the belts, possible flow instabilities and regions of secondary flow near the pulleys all had to be thoroughly investigated.

2.2. *Fluid properties*

Care was taken in the selection of a suitable fluid for use in these experiments. Since it was desirable to operate the shear tank at as high a Reynolds number as could reasonably be obtained, water seemed an obvious choice. However, for a kinematic viscosity of 1 cS, the shear rate beyond which the thickness of the boundary layer on each belt becomes less than half the channel gap width was estimated to be approximately equal to the minimum rate of shear below which the cylinder or sphere cannot freely rotate about its wire support (see § 3 for a detailed discussion of the test objects and support assembly). Also, it was desirable to take photographs of streamline patterns but was difficult to find tracers which, in water, could travel a reasonable length of the channel and still not rise, fall or disappear over the time scale involved (hydrogen bubbles failed to work). Hence a fluid was needed which was more viscous than water and which could easily support a suitable tracer.

An insulating oil manufactured by the Chevron Chemical Company and usually used in transformers, etc., was finally selected as the test fluid. It has a kinematic viscosity of about 17 cS at room temperature and is transparent and almost colourless, thus being quite suitable for photographic purposes.

2.3. *Experimental procedure*

Of primary interest with reference to the present set of experiments was the development of a steady simple shear flow having no mean velocity at the centre of the channel. Thus the belts were run with equal but opposite velocities as shown in figure 2. (Primed quantities are dimensional.) The belts are separated by a distance H and are taken to move in opposite directions with speed U_B. The velocity profile $u'(y')$ set up by such a flow can then be expressed as

$$u'(y') = (2U_B/H)\, y'. \tag{2.1}$$

Thus the dimensional rate of shear S' is given by

$$S' \equiv du'/dy' = 2U_B/H. \tag{2.2}$$

Ideally, one would like to obtain this flow throughout the length of the channel; however, owing to equipment limitations, this is not always possible. The rest of this section is devoted to investigating the degree to which a simple shear as given by (2.1) can be produced in the tank.

Several dimensionless groups will prove useful in characterizing the flow in the test channel, which depends on the values chosen for the two length scales. For the empty tank, a shear Reynolds number Re_T, based on the channel half-width $\frac{1}{2}H$, is defined as

$$Re_T \equiv S'(\tfrac{1}{2}H)^2/\nu = U_B H/2\nu. \tag{2.3}$$

Also, the aspect ratio Λ ($\equiv L/H$, where L is the centre-to-centre pulley distance) is important in determining the nature of the flow in the empty test section. Furthermore, with a cylinder or sphere in the channel, a shear Reynolds number Re, based on the particle radius a, can be defined as

$$Re \equiv S'a^2/\nu = 2U_B a^2/H\nu. \tag{2.4}$$

We also note that $Re = Re_T \kappa^2$, where $\kappa \equiv 2a/H$. The parameter κ will become important later when the effects of the wall on the rotation of and flow around the test object are examined.

In order to minimize bottom effects, the tank was partly filled with 250 gallons of de-ionized water, on top of which was floated a 200 gallon layer of the insulating oil (about $9\frac{1}{2}$ in. deep). Also, we adapted much of the equipment and procedures described by Robertson & Acrivos (1970) to obtain photographs of the streamlines as well as velocity profiles (for further details, see Poe 1975).

Several types of tracer were considered for use in the photographic work. Very tiny air bubbles were judged unsuitable since they rose too quickly in the rather low viscosity oil. Various brands of plastic particle were then carefully examined. A polypropylene product called 'Hercoflat', manufactured by Hercules Chemicals and usually used for texturing and adding pigment to industrial coatings, was found to be quite satisfactory for use as a tracer in the present experiments. Hercoflat no. 1200, having an average particle size of about 200 μm, was the smallest particle visible on the photographic films used here. Also, the settling velocity of these particles (specific gravity about 0·9) was quite small. They settled to the bottom of the oil only after a period of about 12 h.

The camera was mounted at the top of the shear tank, and pictures were taken of the flow between the two moving belts. Tracer particles were first introduced into the channel and illuminated at right angles to the camera by two flashing stroboscopes situated at the end windows of the tank. Using exposure times of about half a minute and the flashing strobes as the only illumination, a photographic tracing of the streamlines was recorded on film. The resulting pictures were very similar to figure 2 of Robertson & Acrivos (1970), who used a much larger channel width ($H = 21{\cdot}25$ in.) and a much more viscous oil ($\nu = 325$ cS at room temperature), and revealed the existence of a recirculating flow region near the centre-line of the test section. As Robertson & Acrivos point out, this behaviour is partly due to the fact that the shear tank is of finite length and has two solid walls at either end, which force some of the fluid passing through the channel to return and flow through the section again. Also, the large centrifugal forces found near the pulleys might be expected to, effectively, partly block off the ends of the channel, thus confining the flow even further. It is clear, though, that the width of this recirculating region should definitely decrease upon decreasing the gap width H. Thus, since a gap width of 6 in. or less was to be used here, it was hoped that the flow in the narrow recirculating region would not be strong enough to disrupt the planned experiments. However, as will be seen later on, this recirculating region did in fact affect the outcome of some of the experiments.

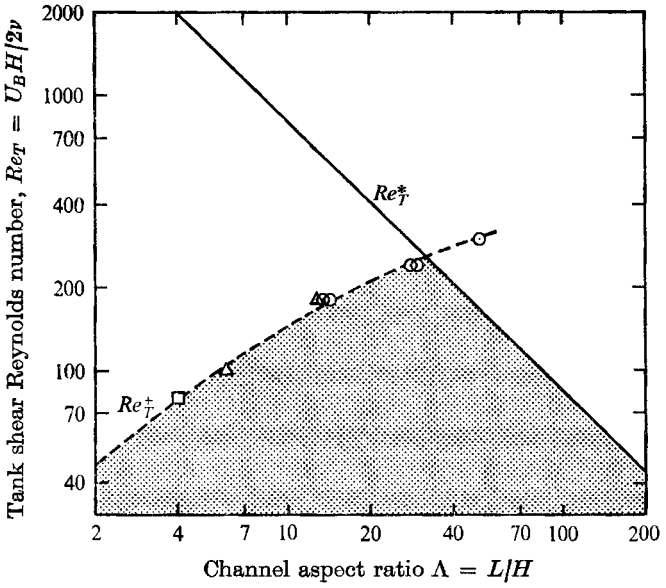

FIGURE 3. Tank shear Reynolds number *vs.* channel aspect ratio showing the various flow regimes in the empty channel: – – –, boundary between linear and nonlinear velocity profile; ——, boundary between presence and absence of Goertler vortices. □, Robertson (1969); △, Kohlman (1963); ⊙, present study.

Belt gap width, H (in.)	Channel aspect ratio, $\Lambda \equiv L/H$ (L = 79 in.)	$Re_{max} = Re_T(2a/H)^2$
19·8	4·0	0·05
13·1	6·0	0·2
6·0	13·2	1·2
2·81	28·1	7·6
2·7	29·3	8·2
1·58	50·0	17
1·0	79·0	26

TABLE 1. Values of Re_{max}

2.4. *The velocity profile of the undisturbed flow*

A large number of experiments were performed to determine the conditions under which the velocity profile in the centre of the empty channel, i.e. in the absence of the cylinder or the sphere, conformed to (2.1). As expected, a linear profile was achieved only as long as Re_T remained below a 'critical' value. This critical value Re_T^* was found to depend on the aspect ratio Λ. In addition, however, a clearly defined secondary vortex flow pattern was observed at the higher belt speeds. This originated near the pulleys and was identified as being due to the generation of Goertler vortices. Of course, it is well known that instabilities leading to secondary motion can arise in flow past a stationary concave wall (cf. Taylor 1923; Dean 1928; Goertler 1940, 1941), but the same type of disturbance can also

occur in the case of a convex wall moving through a stagnant fluid (as in the present study). In fact, linear stability analysis yields identical disturbance equations in both cases (see Lin 1966, pp. 96 ff.; Chandrasekhar 1961, pp. 318 ff.).

In our set-up, these Goertler vortices were formed near the pulleys and immediately carried downstream by the primary flow between the belts. In fact, these vortices were clearly visible near the centre of the channel for values of U_B greater than about 5·5 cm/s. Thus, a second 'critical' Reynolds number Re_T^+ (which by definition is obviously proportional to H) can be computed from this 'critical' value of U_B.

The data from the present experiments together with the earlier results of Robertson (1969) and of Kohlman (1963) were used to construct figure 3, which delineates four distinct flow regimes in the empty tank. Clearly, however, one could be assured of obtaining a truly two-dimensional simple shear as given by (2.1) only if the tank were operated within the shaded portion of figure 3, and hence the experiments to be described in the next section were performed with values of Re_T mainly confined to this region. For the sake of completeness, we report in table 1 the maximum particle Reynolds number $Re_{\max}$, based on the radius a of the test object [cf. (2.4)], beyond which it would have been undesirable to operate the channel for the reasons explained above. A particle radius of 0·25 in. was used in calculating the values of $Re_{\max}$ in table 1. Since 1·58 in. is the minimum value of H which the present shear-flow apparatus allows, we concluded that $Re \approx 17$ is the maximum particle shear Reynolds number that could be attained with the present system without forsaking the linearity of the velocity profile or the absence of secondary motions between the belts. In order to achieve a higher value of $Re_{\max}$ at any given H, we would have had to design an apparatus having a greater channel length L (79 in. here) and/or a larger pulley diameter (about 4 in. here).

3. Simple shear flow past a cylinder and a sphere freely rotating at moderate Reynolds numbers

3.1. *Rates of rotation*

The cylinder and its support assembly are shown in figure 4. The cylinder itself was an 8 in. section of $\frac{1}{2}$ in. O.D. polypropylene tubing having a wall thickness of $\frac{1}{8}$ in. As shown in figure 4, two tightly fitting $\frac{1}{4}$ in. O.D. Delran plugs, through which 0·012 in. diameter holes had been drilled, were inserted in each end. The cylinder was allowed to rotate about a tightly stretched length of nickel wire (200 μm in diameter) which passed through the central holes in the Delran plugs. In anticipation of the need to be able to remove these plugs, two holes $\frac{1}{16}$ in. in diameter were drilled and threaded in the top plug. During an experiment, these holes were sealed with two machine-made plastic screws. Then, to remove the top plug, the two plastic screws were replaced by 1 in. long stainless-steel screws, which acted as a handle with which to pull out the plug.

The wire support assembly and its location in the shear tank are also shown in figure 4. An $\frac{1}{8}$ in. thick 8 × 8 in. piece of lucite was supported over the centre of the

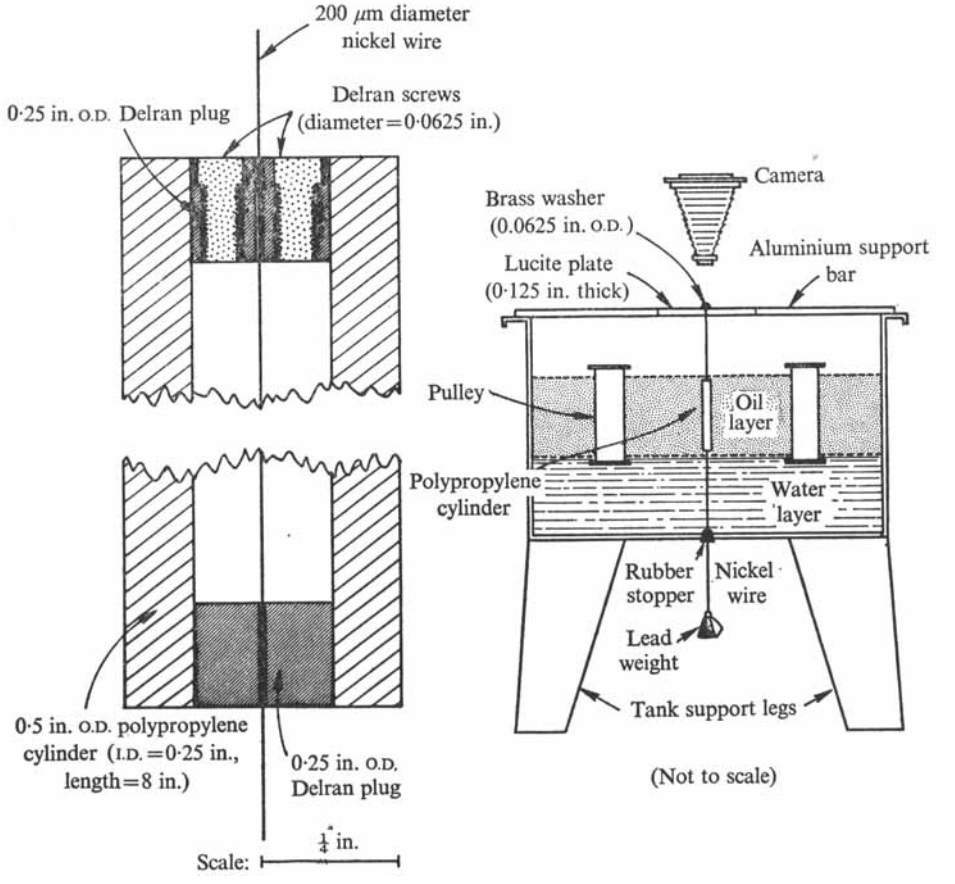

FIGURE 4. Cylinder assembly and its location in the shear-flow apparatus.

channel by an aluminium bar spanning the width of the tank. The nickel wire, which had been passed through the cylinder, was inserted through this lucite plate and secured on top with a tiny brass washer. The other end of the wire passed through a rubber stopper which had been inserted in a hole $\frac{1}{2}$ in. in diameter in the bottom of the tank. The wire was then stretched tightly by hanging a lead weight from its end.

Unfortunately, the cylinder was not only free to rotate about the wire axis, but was also free to slide up and down the wire. In order to prevent this from occurring during an experiment, the following procedure was adopted. The hollow portion $\frac{1}{4}$ in. in diameter inside the cylinder (see figure 4) was partially filled with oil. Since the density of the cylinder assembly (0·916 g/cm^3) was slightly greater than that of the oil, the cylinder would immediately slide down the wire and come to rest in the water layer if its interior were completely filled. Hence, by only partially filling the cylinder interior (i.e. by leaving some air inside it), one could easily regulate the depth at which the cylinder came to rest. However, since oil slowly seeped into the interior through the two central holes at the top and bottom, the cylinder did eventually slide down the wire and partly floated in the water. But

H = 2·81 in.		H = 2·70 in.		H = 1·58 in.	
Re	2Ω	Re	2Ω	Re	2Ω
0·491	0·915	1·50	0·832	3·87	0·657
0·856	0·890	2·02	0·799	5·61	0·618
0·878	0·873	2·28	0·775	6·77*	0·592
1·43	0·845	4·00	0·678	8·53*	0·503
1·45	0·857	5·74	0·580	9·75*	0·528
1·91	0·812	7·49*	0·511	11·5*	0·565
1·97	0·822	8·88*†	0·464	12·4*	0·585
2·47	0·770			14·7*	0·555
3·57	0·696			18·2*†	0·513
4·36	0·624			21·1*†	0·456
5·60	0·622				
6·36*	0·602				
7·54*	0·498				
8·27*†	0·472				
9·84*†	0·400				

TABLE 2. Values of 2Ω for the cylinder

this occurred over a period of 1–2 h and hence there was ample time to obtain measurements and photographs while the cylinder remained totally immersed in the oil layer.

The effect of the wire and the presence of both air and oil in the interior of the cylinder had to be properly taken into account when calculating the angular velocity from the measured rate of rotation. However, a torque balance on the interior cylinder assembly showed that these effects were entirely negligible and that no significant corrections were needed when calculating the angular velocity. With the cylinder spanning almost the entire depth of the oil layer, it was expected that the effect of its finite length on the measurements would also not be very significant. Of course, all these effects remained to be tested.

A similar set-up was also used for the sphere (Poe 1975).

Only three gap widths were used in this set of experiments: H = 2·81, 2·70 and 1·58 in. The belt speed U_B was varied from 0·27 to 7·0 in./s, while the shear rate S' ranged from 0·2 to 8·9 s^{-1}. The kinematic viscosity of the oil was always found to lie between 14 and 20 cS, while the particle shear Reynolds number Re, computed from (2.4), varied from about 0·5 to 20. The angular velocity Ω was determined by measuring the time (Δt) required for the particle to make N revolutions. Five to fifteen measurements of $N/\Delta t$ were made at each Reynolds number, and the average value was used in calculating Ω (the standard deviation was generally 1–2 % in each case). Summaries of the experimentally determined Ω's are reported in table 2 for the cylinder and in table 3 for the sphere.

Some unusual behaviour was noticed when operating the belts at particle Reynolds numbers greater than about 6 or 7. Both the cylinder and the sphere were observed to rotate rather unevenly, i.e. one could actually detect the objects speeding up and slowing down by simply observing the rotating motion of a black dot painted on them. Obviously, at these values of Re, significantly different

H = 2·81 in.		H = 2·70 in.		H = 1·58 in.	
Re	2Ω	*Re*	2Ω	*Re*	2Ω
0·780	0·976	5·32	0·803	3·82	0·825
0·793	0·943	6·31*	0·837	5·48	0·835
0·803	0·954	6·94*	0·765	6·61*	0·821
1·23	0·935	8·23*†	0·760	8·38*	0·811
1·31	0·970			9·57*	0·827
1·33	0·962			12·4*	0·837
1·65	0·945			14·7*	0·821
1·77	0·933			18·2*†	0·785
1·80	0·923			21·1*†	0·794
1·93	0·921				
2·08	0·907				
2·69	0·905				
2·98	0·885				
3·26	0·865				
3·50	0·844				
3·59	0·861				
4·15	0·837				
4·55	0·845				
4·77	0·836				
5·14	0·824				
5·19	0·852				
5·68	0·843				
6·11*	0·880				
6·23*	0·877				
6·56*	0·867				
6·69*	0·813				
7·73*†	0·728				
7·91*†	0·643				

TABLE 3. Values of 2Ω for the sphere

values of $N/\Delta t$ could be measured depending on when the measurements were taken and on how large a value of N was used. Hence a considerable amount of scatter was found in the data. For these tests (marked with an asterisk in tables 2 and 3), the standard deviation in the 2Ω values jumped to ± 3–10 %.

Also, as discussed in an earlier section, for a given gap width H, there was a maximum value of Re (denoted by $Re_{\max}$) below which one was assured of having a linear profile in the centre of the test section and no secondary flow (see table 1). For H = 2·81, 2·70 and 1·58 in., $Re_{\max}$ was found to be equal to 7·6, 8·2 and 17, respectively. Some of the data in tables 2 and 3 were obtained at Reynolds numbers above these values. These tests are marked with a dagger.

3.2. *Discussion and comparison with theory*

The results presented in table 2 are plotted in figure 5 and those in table 3 in figure 6. Those data having both an asterisk and a dagger beside them in tables 2 and 3 are plotted here as diamonds, while those having only an asterisk are denoted by squares in these graphs. Open circles are used for the remainder of the data.

It may be seen in both figure 5 and figure 6 that, for $Re > 6$, the scatter in the

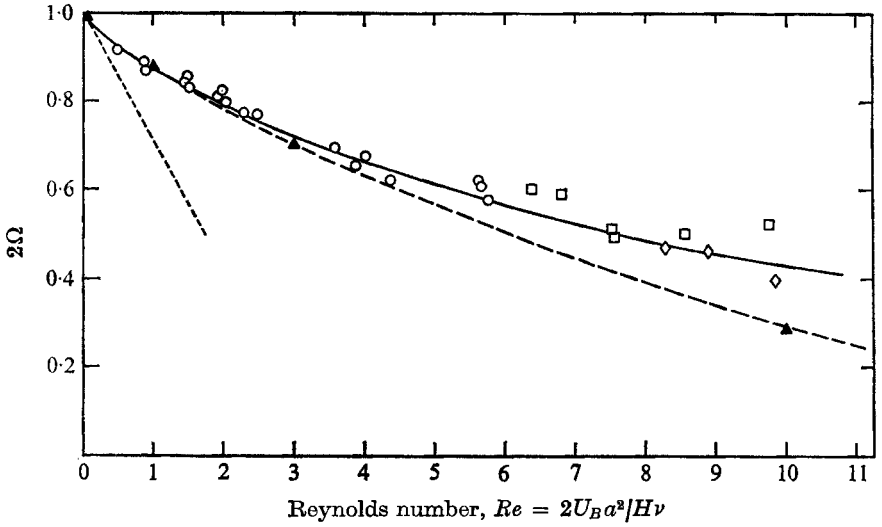

FIGURE 5. Angular velocity *vs.* Reynolds number for a freely rotating cylinder in a simple shear. – – –, $2\Omega \to 1 - 0{\cdot}289Re$ as $Re \to 0$, Robertson & Acrivos (1970); ▲, — —, Kossack & Acrivos (1974); ○, ◇, □, ——, present experiments.

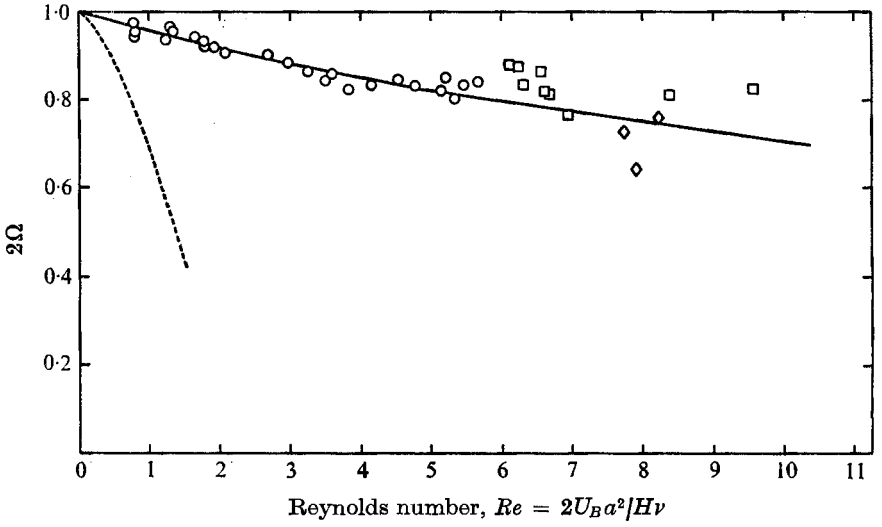

FIGURE 6. Angular velocity *vs.* Reynolds number for a freely rotating sphere in a simple shear. – – –, $2\Omega \to 1 - 0{\cdot}308Re^{\frac{3}{2}}$ as $Re \to 0$, Lin *et al.* (1970); ○, □, ◇. ——, present experiments.

experimentally obtained values of 2Ω is considerably greater than for $Re < 6$. In addition, as discussed earlier, since both the cylinder and the sphere were observed to rotate rather unevenly beyond $Re \sim 6$, different values of Ω could be obtained depending upon when a measurement was taken and how many revolutions were used in a test. Also, in both cases, this uneven rate of rotation was found to correspond to unsteady motion; i.e. there was no regular pattern to the speeding up and slowing down of the rotating cylinder or sphere. In fact,

photographs taken of the streamline patterns around the object (to be discussed later) revealed that, in both cases, beyond $Re \sim 6$ the two wakes found on either side of the object behaved, at times, in an unsteady fashion; i.e. these wakes tended to oscillate about the imaginary centre-line of the channel in an irregular manner. These observations suggest that the motion about a cylinder or sphere freely rotating in a simple shear is steady only up to a Reynolds number of about 6.

It may also be seen from figure 5 that, for $Re < 5$, the experimentally determined curve of 2Ω *vs.* Re agrees rather well with the curve obtained by connecting the data of Kossack & Acrivos (1974),† who computed numerical solutions to the full Navier–Stokes equations for a freely rotating cylinder in a simple shear. However, for values of Re greater than about 5, the experimental curve is seen to deviate slightly from that derived numerically. One possible explanation for this deviation is described below.

As discussed at the end of § 2.3, the narrow recirculating flow region found in the empty channel may cause a slight increase in the rate of rotation of the cylinder at the higher Reynolds numbers, since as the belt speed U_B is increased, the large centrifugal forces acting on the fluid flowing around the pulleys, effectively, partly block off the ends of the channel, thus confining the flow even further. Photographs taken of the flow near one of the pulleys in order to test this revealed that the amount of fluid completely bypassing the channel increased as the belt speed was increased. Thus the two ends of the channel were, for the most part, blocked off and a rather wide recirculating flow was observed at these locations, even though photographs taken near the centre of the channel showed that the width of this recirculating flow region was much less and that the velocity profile was indeed linear.

For the same reason, one might also expect the values of 2Ω for the sphere shown in figure 6 to be slightly high for $Re > 5$. However, since results similar to those of Kossack & Acrivos (1974) do not exist for the sphere, no other data are available for the purposes of comparison. Nevertheless, this point should be kept in mind when dealing with the data taken beyond Reynolds numbers of about 5.

An additional factor to consider is the close proximity of the two walls to the surface of the body and its effect on the rate of rotation of the cylinder or the sphere. In the present experiments, the parameter $\kappa (\equiv 2a/H)$ ranged from 0·18 to 0·32. For $Re \ll 1$, Ho & Leal (1974) found that a small sphere placed in a simple shear between two walls rotates with the vorticity of the fluid to within a very small correction, $O(\kappa^3)$ for $\kappa \ll 1$, which would be negligible in our case. However, since no analysis comparable to that of Ho & Leal exists for values of Re beyond the Stokes range, predictions concerning the wall correction for Ω cannot be made for $Re \neq 0$. Nevertheless, upon examining the data given in tables 2 and 3, one finds, in both cases, that for a fixed value of Re (< 6) the value of Ω at one gap width H is not significantly different from its value at another H. Hence, for Re up to about 6, the wall effect on Ω appears to be small, at least for values of κ up to 0·32.

† In figure 5, the numerically computed value of 2Ω at $Re = 3{\cdot}0$ was obtained later by Kossack (private communication).

Another point to consider is that the disturbance to the primary flow caused by freely suspending a sphere in the centre of a simple shear flow is expected to be smaller than that resulting from an 'infinitely' long cylinder of the same diameter. This is borne out by comparing the data in figures 5 and 6, from which it is seen that, with increasing Re, Ω does not decrease as rapidly for the sphere as it does for the cylinder. In fact, in the case of the sphere, 2Ω remained larger than 0·5, even for values of Re as high as 10.

Also shown in figures 5 and 6 are the asymptotic solutions for $Re \ll 1$ obtained analytically by Robertson & Acrivos (1970) for a cylinder and by Lin *et al.* (1970) for a sphere. In both cases, it is immediately clear that beyond a Reynolds number of about 0·1 these analytic solutions no longer agree with the experimentally determined values of Ω.

3.3. *The streamline patterns*

Photographs of streamline patterns around the cylinder and the sphere were obtained using the illumination technique described in § 2.3. Except when noted, all photographs were taken 3 in. below the top surface of the oil.

A typical photograph of the flow around a freely rotating cylinder is shown in figure 7 (plate 1), where the halo effect was caused by the reflexion of light from the two flashing strobes off the white surface of the cylinder. Also, owing to the close proximity of the top end of the cylinder to the camera lens, the cylinder sometimes looked out of focus. Still, a large portion of the streamline pattern was clearly visible in most of the photos.

Figure 8 (plate 1) depicts the flow around a freely rotating sphere. Photos were taken only in the mid-plane of the sphere, since the streamlines above and below this plane are three-dimensional. The quality of the photos here was generally much better than in the case of the cylinder, owing to the decreased amount of light reflected off the smaller surface of the sphere.

Besides the fact that each body is surrounded by a region of closed streamlines, the most striking feature of both photos is the presence of two stagnation points followed on either side of the body by two recirculating wakes. Owing to the extremely slow motion in the neighbourhood of a stagnation point, it was sometimes very difficult to obtain photographs of tracer particles in these regions; nevertheless one could easily discern the locations of the stagnation points in most of the photos.

In order to obtain a quantitative comparison between the experimental results found here for the cylinder and the numerical predictions of Kossack & Acrivos (1974), the distance r_s from a stagnation point to the centre of the cylinder was measured on those photos where such a point was clearly visible. These results were then plotted (see figure 9) and compared with the curve obtained by connecting the numerically found values of Kossack & Acrivos. Although data were not taken over the entire range, it is clear from figure 9 that there is fairly good agreement between the two sets. Also shown for comparison is the asymptotic expression for $Re \ll 1$:

$$r_s \to 1{\cdot}127 Re^{-\frac{1}{4}}\{1 + O[Re(\ln Re)^2]\} \quad \text{as} \quad Re \to 0,$$

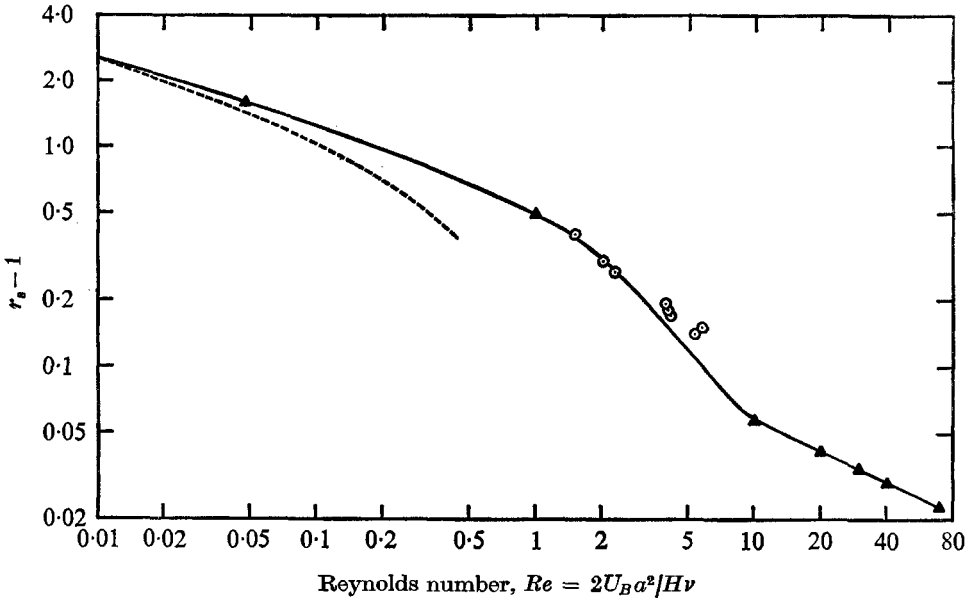

FIGURE 9. Stagnation-point location for a freely rotating cylinder in a simple shear. – – –, $r_s - 1 \to 1{\cdot}127Re^{-\frac{1}{2}} - 1$ as $Re \to 0$, Robertson & Acrivos (1970); ▲, ——, Kossack & Acrivos (1974); ⊙, present experiments.

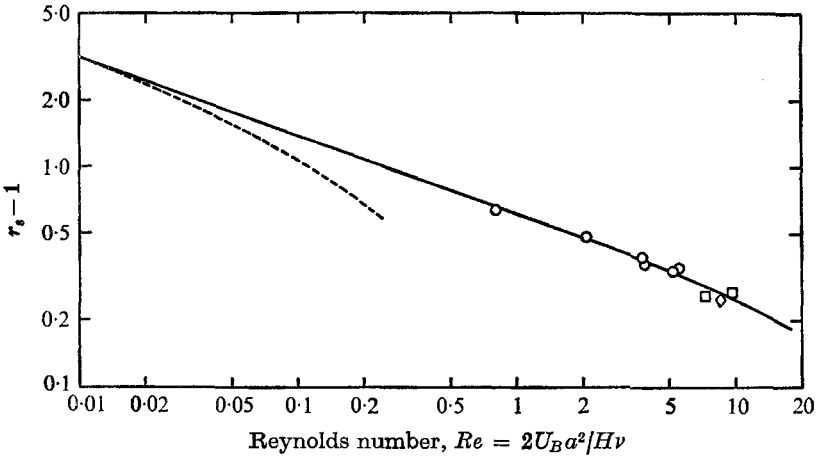

FIGURE 10. Stagnation-point location for a freely rotating sphere in a simple shear. – – –, $r_s - 1 \to 1{\cdot}034Re^{-\frac{3}{10}} - 1$ as $Re \to 0$, Lin *et al.* (1970); ○, □, ◇, ——, present experiments.

which was derived (Poe 1975) from the analytic solution of Robertson & Acrivos (1970).

The corresponding measurements of r_s for the sphere are plotted in figure 10, together with the asymptotic expression

$$r_s \to 1{\cdot}034Re^{-\frac{3}{10}}[1 + O(Re^{\frac{13}{10}})] \quad \text{as} \quad Re \to 0$$

derived by Poe (1975) from the analytic solution of Lin *et al.* (1970). Since it was found previously that, with increasing Re, Ω did not decrease as rapidly for the

sphere as it did for the cylinder, one would expect that, likewise, the stagnation point would not approach the surface as rapidly for the sphere as for the cylinder. It is clear from the experimental curves in figures 9 and 10 that this is indeed the case.

Streamline photos were also taken for the case $\Omega = 0$, using the technique described earlier. The cylinder was held stationary by attaching to the wire two small weights, one just above and the other just below the cylinder. With the two weights pressed against its top and bottom, the cylinder could not rotate. The sphere was similarly fixed. Generally, the quality of the photos was not as good as that found previously; none the less one could still discern the main features of the flow pattern from most of them. Two of these photos are presented in figures 11 and 12 (plate 2). For both the cylinder and the sphere, one finds, in this case, a complete absence of closed streamlines and the presence of four stagnation points, all lying on the surface of the body. These stagnation points are partially visible in the photographs presented here.

This work was supported in part by the National Science Foundation under grant NSF-GK-41781. The oil used in the experiments was generously donated by the Chevron Chemical Company.

REFERENCES

Bretherton, F. P. 1962 Slow viscous motion round a cylinder in a simple shear. *J. Fluid Mech.* **12**, 591.

Chandrasekhar, S. 1961 *Hydrodynamic and Hydromagnetic Stability*. Oxford: Clarendon Press.

Cox, R. G., Zia, I. Y. Z. & Mason, S. G. 1968 Particle motions in sheared suspensions. XXV. Streamlines around cylinders and spheres. *J. Colloid Interface Sci.* **27**, 7.

Darabaner, C. L., Raasch, J. K. & Mason, S. G. 1967 Particle motions in sheared suspensions. XX. Circular cylinders. *Can. J. Chem. Engng*, **45**, 3.

Dean, W. R. 1928 Fluid motion in a curved channel. *Proc. Roy. Soc.* A **121**, 402.

Goertler, H. 1940 Über eine dreidimensionale Instabilität laminarer Grenzschichten an konkaven Wänden. *Nachr. Ges. Wiss. Göttingen*, **2**, 1.

Goertler, H. 1941 Instabilität laminarer Grenzschichten an konkaven Wänden gegenüber gewissen dreidimensionalen Störungen. *Z. angew. Math. Mech.* **21**, 250.

Ho, B. P. & Leal, L. G. 1974 Inertial migration of rigid spheres in two-dimensional unidirectional flows. *J. Fluid Mech.* **65**, 365.

Kohlman, D. L. 1963 Experiments on cylinder drag, sphere drag and stability in rectilinear Couette flow. *M.I.T. Fluid Dyn. Res. Lab. Rep.* no. 63–1.

Kossack, C. A. & Acrivos, A. 1974 Steady simple shear flow past a circular cylinder at moderate Reynolds numbers: a numerical solution. *J. Fluid Mech.* **66**, 353.

Lin, C. C. 1966 *The Theory of Hydrodynamic Stability*. Cambridge University Press.

Lin, C. J., Peery, J. H. & Schowalter, W. R. 1970 Simple shear flow round a rigid sphere: inertial effects and suspension rheology. *J. Fluid Mech.* **44**, 1.

Poe, G. G. 1975 Closed streamline flows past rotating particles: inertia effects, lateral migration, heat transfer. Ph.D. thesis, Stanford University.

Proudman, I. & Pearson, J. R. A. 1957 Expansions at small Reynolds numbers for the flow past a sphere and a circular cylinder. *J. Fluid Mech.* **2**, 237.

Raasch, J. K. 1961 Das Verhalten suspendierter Feststoffteilchen in Scherströmungen hoher Zähigkeit. *Z. angew. Math. Mech.* **41**, 147.

ROBERTSON, C. R. 1969 Low Reynolds number shear flow past a rotating circular cylinder: momentum and heat transfer. Ph.D. thesis, Stanford University.

ROBERTSON, C. R. & ACRIVOS, A. 1970 Low Reynolds number shear flow past a rotating circular cylinder. Part 1. Momentum transfer. *J. Fluid Mech.* **40**, 685.

SAFFMAN, P. G. 1965 The lift on a small sphere in a slow shear flow. *J. Fluid Mech.* **22**, 385.

TAYLOR, G. I. 1923 Stability of a viscous liquid contained between two rotating cylinders. *Phil. Trans.* A **223**, 289.

TAYLOR, G. I. 1934 The formation of emulsions in definable fields of flow. *Proc. Roy. Soc.* A **146**, 501.

TREVELYAN, B. J. & MASON, S. G. 1951 Particle motions in sheared suspensions. I. Rotations. *J. Colloid Sci.* **6**, 354.

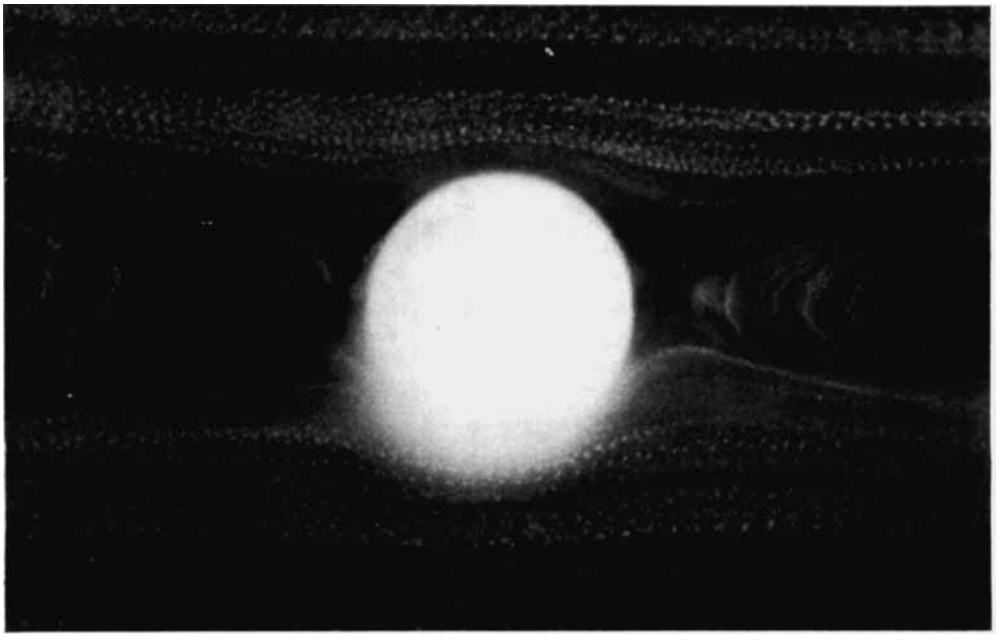

FIGURE 7. Shear flow past a freely rotating cylinder:
$H = 2{\cdot}70$ in., $U_B = 1{\cdot}27$ in./s, $Re = 2{\cdot}28$.

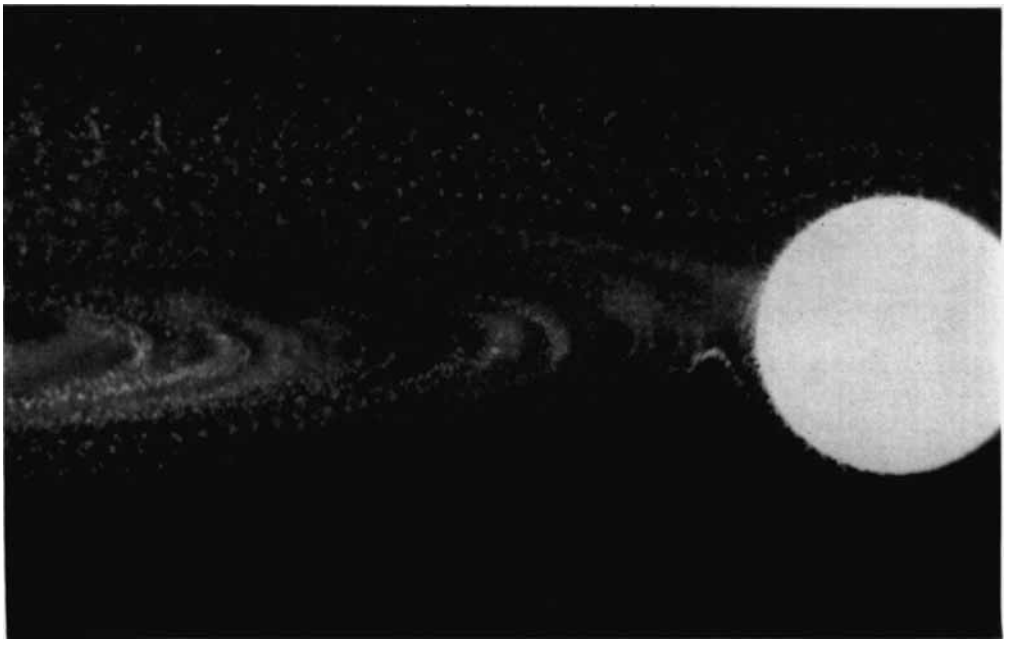

FIGURE 8. Shear flow past a freely rotating sphere:
$H = 2{\cdot}81$ in., $U_B = 3{\cdot}19$ in./s, $Re = 5{\cdot}13$.

(*Facing p.* 624)

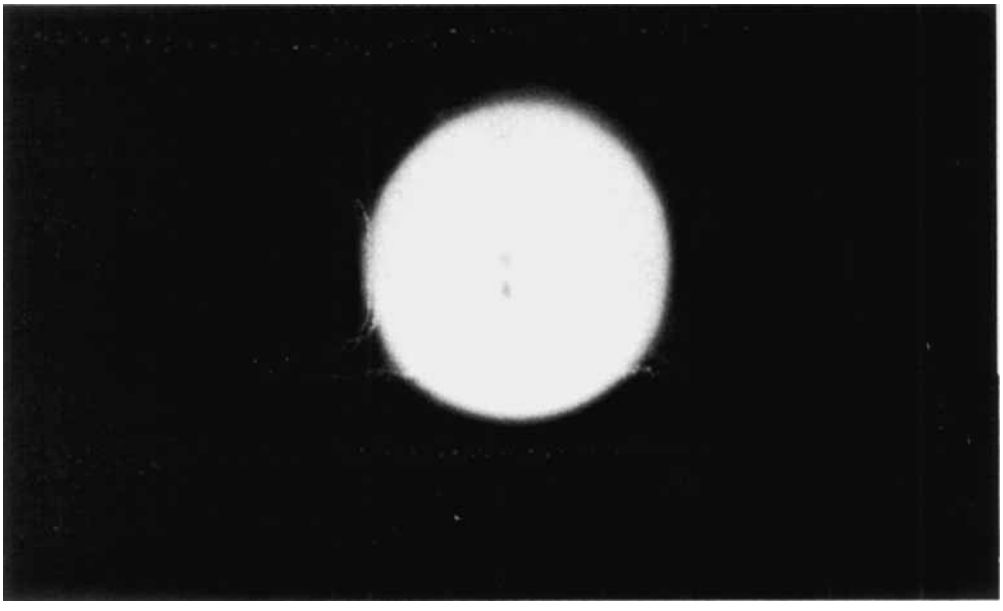

FIGURE 11. Shear flow past a stationary cylinder:
$H = 2{\cdot}70$ in., $U_B = 1{\cdot}27$ in./s, $Re = 2{\cdot}22$.

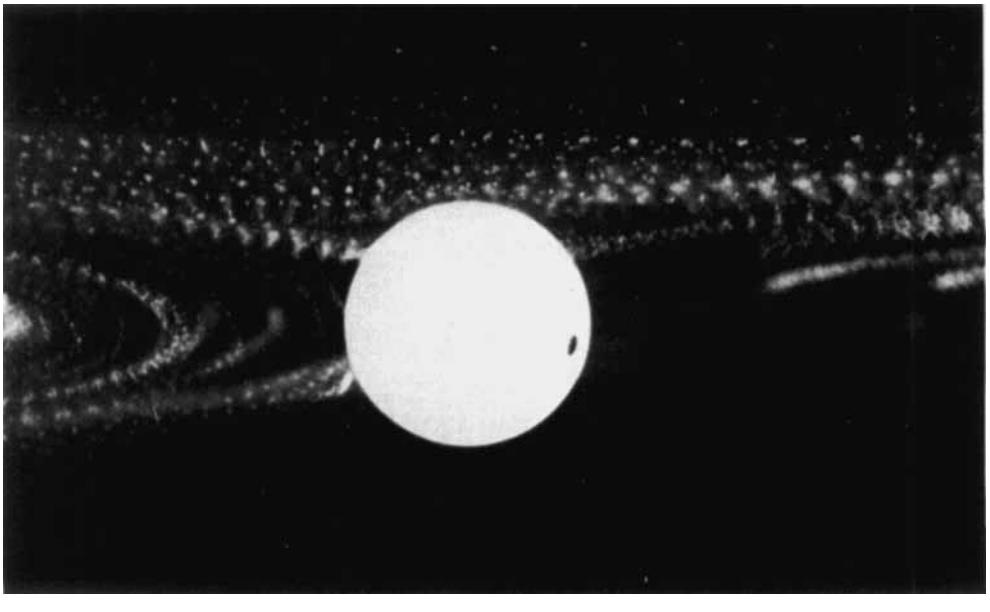

FIGURE 12. Shear flow past a stationary sphere:
$H = 2{\cdot}70$ in., $U_B = 1{\cdot}27$ in./s, $Re = 2{\cdot}14$.